This is a preprint, the final version is subject to change, of the American Mineralogist (MSA)
Cite as Authors (Year) Title. American Mineralogist, in press.
DOI: https://doi.org/10.2138/am-2018-6131

VERSION 3

Insight on gem opal formation in volcanic ash deposits from a supereruption: a case study through oxygen and hydrogen isotopic composition of opals from Lake Tecopa, California, USA.

Erwan Martin[1], Eloïse Gaillou[2]

[1] Sorbonne Université, CNRS-INSU, Institut des Sciences de la Terre Paris, ISTeP UMR 7193, F-75005 Paris, France.
[2] MINES ParisTech, PSL Research University, Musée de Minéralogie, 60 boulevard Saint-Michel, 75006 Paris, France.

Abstract

At Lake Tecopa, in California, white play-of-color opals are found in vesicles of a volcanic ash layer from the Huckleberry Ridge Tuff super-eruption (2.1 Ma). They show characteristic traits of opal-AG by X-ray diffraction and scanning electron microscopy (silica spheres of ~330 nm). These properties are not typical for volcanic opals, and are usually associated with opals formed in a sedimentary environment, such as opal-AG from Australia. The conditions under which opal was formed at Lake Tecopa were determined by oxygen and hydrogen isotopic analyses and lead to a better understanding of the formation of opal in general.

Tecopa opal's $\delta^{18}O$ is ~ 30 ‰, leads to a formation temperature between 5°C and 10°C from water composition similar to the present spring water composition ($\delta^{18}O$ = -12‰), or between 15°C and 30°C (the present day spring water temperatures) in water having a $\delta^{18}O$ between -9.5 and -5.5‰, and as a result experienced 25-50% evaporation at the Tecopa basin. Contrary to long-held views, the formation of opal-AG versus opal-CT (or opal-C) is not determined by the type of deposits, i.e. respectively sedimentary versus volcanic, but mostly by the temperature of formation, low (≤ 45°C for opal-AG) versus high (≥ 160°C for opal-CT) as suggested in most recent papers.

The isotopic composition of water contained in Tecopa opals is assessed and results show that water in opal records different stages of opal formation from groundwater. Opal seems to precipitate from groundwater that is undertaking isotopic distillation during its circulation, most likely due to 15% up to 80-95% evaporation. Hydrogen isotopes are poorly documented in opal and require more systematic work, but this study reveals that, in Tecopa opals, molecular water (H_2O_m) is isotopically heavier than structural water (OH), (a phenomena already well-known in amorphous volcanic glass). Overall, opal isotopic composition reflects the composition of the water from which it precipitated and for that reason could be, (as established for amorphous silicic glass), a useful tool for paleoenvironments, and paleoclimatic reconstitutions on Earth and on other terrestrial planets.

Introduction

The formation mode of opal, which is an amorphous to poorly crystalline hydrated silica, has mostly been studied in biogenic samples, such as diatoms, because of their importance in the silicon cycle in oceans, past and present (e.g. De La Rocha et al., 1998). Hot Spring opals have been used as possible proxy for the study of early life on Earth and life on Mars (e.g. Jones & Renaut, 2007 and the review paper by Campbell et al., 2015). These opals are not gem quality, as they are highly porous, and lack color and play-of-colors (iridescence). In contrast, gem opals are valued because of their body color (i.e. background color), transparency and / or the presence of play-of-color. Unlike biogenic opals, they do not form in oceans, but on continents by weathering of silica-rich rocks either in a sedimentary or a volcanic environment (e.g., Des Cloizeaux, 1862; Lacroix, 1896; Payette, 1999; Gaillou et al., 2008a, Rondeau et al., 2012; Rey, 2013). As opal contains water in the form of both H_2O and OH, hydrogen and oxygen isotopic analyses can be conducted in order to understand its formation mode.

At the dry Lake Tecopa, California, play-of-color opal is present in nodules within a volcanic ash layer from a Yellowstone supereruption (Huckleberry Ridge Tuff, 2.1Ma; e.g. Rivera et al. 2014). The purpose of this study is to use Lake Tecopa play-of-color opals in order to better understand the processes that lead to the formation of gem opals. We present oxygen and hydrogen isotope measurements on Tecopa opals and their host rock, which allow the assessment of the formation conditions, such as fluid composition and the temperature from which opal precipitated.

Background on gem opals

Opal can be divided in three structural groups (Jones and Segnit, 1971): opal-C (well-ordered α-cristobalite), opal-CT (disordered α-cristobalite, α-tridymite), and opal-A (nearly amorphous). These groups can be identified by X-ray diffraction (XRD; e.g. Jones and Segnit, 1971) by Raman spectroscopy (e.g. Ostrooumov et al. 1999), by Scanning Electron Microscopy (SEM; Gaillou et al., 2008b) or by Infrared spectrometry (Chauviré et al., 2017). Langer and Flörke (1974) further distinguished opal-AG (with a Gel-like structure) from opal-AN (with a Network-like, or glass-like structure; also called hyalite opal).

Opal-AG is the most well-known, as the most spectacular gem opals are of this type, including Australian opals. Both opal-CT (to opal-C) and opal-AG may show play-of-colors, if they have a structural arrangement at the nanoscopic scale (~150 - 350 nm; Jones et al., 1964) that permits light diffraction. Opal-AG is characterized by a stacking of spheres that may arrange into cubic packing (then showing play-of-color). Gem opal-CT (to opal-C) may have a variety of structures but never shows perfect spheres. However, it may form lepispheres, that when arranged with cubic packing, will display play-of-colors (e.g., Fritsch et al., 1999; Gaillou et al., 2008b).

Not all gem opals show play-of-colors, as they can also be attractive due to their transparency and body colors spanning the entire rainbow. For example, the valuable fire opals have an attractive red color, and the blue opals span a range from sky blue to aqua blue.

Gem quality opal is formed either in sedimentary environments, such as Australia, where the opal forms in veins of sandstones of the Great Artesian Basin (e.g. Rey, 2013), or in a volcanic setting (such as in Mexico) where opal forms in voids created during cooling of ignimbrites and rhyolitic tuffs (e.g. Koivula et al., 1983; Gübelin, 1986).

Opal-AG has long been associated with sedimentary deposits, while opal-C and -CT with volcanic environments (e.g., Smallwood et al., 1997; Ostrooumov et al., 1999; Smallwood, 2000; Smallwood et al., 2008). However, this is not always true and opal-AG and opal-CT may be found in both environments (Rondeau et al., 2004; Gaillou et al., 2008b, Chauviré et al., 2017). Based on a study on oxygen isotopes, Rondeau et al. (2004) suggested that an important parameter in the formation of opal-AG versus -CT is the temperature, rather than the geological setting. This study showed that opal-AG from Australia in a sedimentary deposit and opal-AG from Slovakia in a volcanic setting were formed at temperatures lower than 45°C. In contrast, Mexican opals (mostly opal-CT) formed in a volcanic setting were formed at about 160°C (Spencer et al., 1992).

Geological setting

The presently dry Lake Tecopa is located in the major intermontane basin southeast of Death Valley (Figure 1). During most of its existence from Pliocene to middle Pleistocene, Lake Tecopa oscillated between playa to shallow-lake conditions under arid to semi-arid environments and even during its deepest stages (5-10 m) it remained both saline and alkaline (e.g. Larsen, 2008; Larsen et al., 2001; Morrison, 1999). In this dry lake, the sedimentary deposit is 100 meters-thick and it contains at least 15 ash layers (Hillhouse, 1987; Sheppard

and Gude, 1968; Strakey and Blackmon, 1979). Ash layers were emplaced by air-fall deposits with possible subsequent fluvial re-working and re-deposition from the water catchment area. The three main ash layers that are meter-thick (up to 4 m) and continuously present across the basin are: the 0.63 Ma Lava Creek Tuff, the 2.1 Ma Huckleberry Ridge Tuff from Yellowstone supereruptions and the 0.77 Ma Bishop Tuff from the supereruption that formed the Long Valley caldera (e.g. Crowley et al. 2007; Rivera et al. 2014; Matthews et al. 2015; Martin and Bindeman 2009).

Materials

Opals from this study were collected in a small valley about 10 km south of the town of Shoshone on the West side of the Tecopa basin (N 35°53'20.2"; W 116°15'50.7"). Opals are present in the volcanic ash layer associated with the Huckleberry Ridge Tuff (HRT; Fig. 2). The best outcrops of this volcanic deposit occur in the southern part of the basin. These outcrops consist of hydrous glass shards (3.6wt.% water) that are altered mostly in K-felspar and form a resistant ledge of 10 cm to ~1 m in thickness (Fig. 2). This ash layer is relatively well laminated with undulations at its base (amplitude ~50 cm and wavelength ~1 m) due to loading pressures, turbidity flow or seismic shaking while the deposit was consolidating in the basin (e.g. Hillhouse, 1987). Siliceous clay nodules are also present in this consolidated volcanic layer and opal fills the nodule vesicles (Fig. 2). These vesicles are usually few millimeters to centimeters in size (Fig. 2).

The opal samples that were analyzed for isotopic analyses are from 3 different nodules. The opal 1a and opal 1b are from nodule 1 and opal 2 is from nodule 2 (Table 1). In order to analyze a whole nodule, no opals were extracted from nodule 3 (Table 1). Nodule 4 and 5 were analyzed by SEM and XRD: nodule 4 had less play-of-color areas (called "potch" Opal 4) while nodule 5 was rich in play-of-color (called "poc" Opal 5). Each nodule was broken

into a few millimetric pieces to give fresh surfaces necessary for looking at the microstructure by SEM. One fresh surface each of opal 4 and opal 5 were used for XRD.

Analytical techniques

For XRD investigations, samples were mounted on glass fibers into a Rigaku D/MAX-RAPID microdiffractometer with an imaging plate detector (Smithsonian Institution, Dept. of Mineral Sciences), a Mo tube source (k-alpha1 $\lambda = 0.7093$ Å), with an X-ray tube operating at 50 kV and 40 mA. Samples were rotated 360° around the phi axis at 1° s^{-1} during data collection with a 10 min exposure time. Mineral phases (tridymite versus cristobalite) were identified using the ICDD database.

High-resolution images were obtained with a FEI Nova NanoSEM 600 variable pressure ultra-high resolution scanning electron microscope (SEM), using a current of 15 kV and 2 nA (Smithsonian Institution, Dept. of Mineral Sciences). Two types of samples were imaged for each opal: freshly fractured, and fractured followed by etching in 10 vol. % HF for 30 sec. Samples were coated with ~5 nm of gold-palladium alloy.

Oxygen isotope compositions ($\delta^{18}O$) were measured via the laser fluorination line in the Stable Isotopes Laboratory at the University of Oregon. Between 1 and 2 mg of single or multiple grains of opal (and host rocks) were loaded in the sample chamber where short (30 s, 1 min and 5 min) bromine pentafluorite (BrF_5) pretreatments were performed in order to remove all the water on the surface of the samples. Molecular oxygen was extracted from samples by a 35 W CO_2-laser using BrF_5 as a reagent and purified from the traces of the reagent cryogenically and through the boiling mercury diffusion pump. After conversion into CO_2, the oxygen isotopes were measured on a Finnigan MAT253 mass spectrometer and run in a dual inlet mode. The $\delta^{18}O$ values obtained were normalized to the international standard GMG = 5.75 ‰ (on a VSMOW scale; Gore Mountain Garnet). During the experiments, the

GMG value was 5.67 ± 0.16 ‰ (2σ; N=10). The lower reproducibility than usually observed on this line (< 0.1 ‰; 2σ) is inferred as coming from the fluorination line background that is slightly higher than usual (~0.35 µmol vs. < 0.2 µmol) due to high reactivity of opal and its water with BrF_5.

In order to assess independently oxygen isotopic composition of silica and water in opals, three analytical procedures were used: (1) the oxygen isotopes were measured on pretreated (as described above) opals only. This procedure leads to the composition of the whole opal (silica + total water). (2) Opal samples were dehydrated in a vacuum oven at 250°C during 3 hours before fluorination. As dehydration under vacuum condition prevents isotopic exchange between extracted water and silica at high temperature (e.g. Brandiss et al. 1998), this procedure assesses the composition of silica only. (3) The opal samples were quickly (~30 s) melted using the laser, while water was pumped away. This method allows a rapid and complete dehydration of the opal samples and it also prevents significant isotopic exchange between extracted water and silica at high temperature. As for procedure 2, this third procedure leads to the silica composition only. However, as complete dehydration is a key point, this new procedure is compared to procedure 2, which is the most commonly used.

Good reproducibility of ±0.1 ‰ is observed in the silica $\delta^{18}O$ ($\delta^{18}O_{silica}$) via procedure 2 (dehydration in vacuum oven) and procedure 3 (laser melting; Table 1). This indicates that no significant isotopic exchange occurred during opal dehydration due to water separation from opal during the dehydration process or the isotopic exchange is reproducible between a slow or rapid dehydration process (3 hours vs. ~10 seconds), which is less likely due to possible kinetic isotopic fractionation.

Ash samples hosting the opal nodules as well as the nodule matrix (clay + opal) were also analyzed following procedure 1.

Hydrogen isotope composition (δD) and total water contents were measured using a continuous flow system which consists of a high-temperature conversion elemental analyzer (Finnigan TC/EA) coupled to a Finnigan MAT253 mass spectrometer in the Stable Isotopes Laboratory at the University of Oregon. The δD values obtained were normalized to the international standards such as NBS30 (δD = 50 ‰, H_2O = 3.5 wt%), and in house standards RUH2 (δD = -81.4 ‰, H_2O = 4.5 wt%) and BUD (δD = -144.7 ‰, H_2O = 2.8 wt%; all on a VSMOW scale). It is noteworthy that the δD value of these standards were recently re-calibrated for analyses with the TC/EA-MAT253 system at the university of Oregon (see Martin et al. 2017 for further discussion). During the experiments, the reproducibility of different in house standard was ± 2 ‰ (2σ). Furthermore, this method allows a precise measurement of the water content with a precision ≤ 0.1 wt.% (Martin et al. 2017).

Result

Opal characterization

Opals are observed in vesicles of a consolidated volcanic ash layer. They are white to milky, frequently with play-of-colors (Fig. 2). They are hydrophane (they stick to the tongue), meaning that they are porous. Specific gravity obtained with a hydrostatic scale on two samples were 1.88 and 2.09, which is in the typical range of gem opals (usually between 1.90 and 2.25; Webster, 1975). The total water content is 3.5 - 4 wt.% (Table 2), which is in the low range for gem opals (usually between 3 and 10 wt.%; e.g., Langer and Flörke, 1974; Holzhey, 1997; Day and Jones 2008).

XRD (Fig. 3) demonstrated that both play-of-color and the rarer common (without play-of-colors) opals from Tecopa are opal-AG, as they present a unique broad diffraction feature centered around 4.1 Å (Jones and Segnit, 1971). In the opal-bearing tuff, amorphous phase

(most likely glass), microcline and muscovite were identified, consistent with what was previously observed in the volcanic deposits from the Tecopa basin (e.g. Larsen, 2008).

SEM images showed a structure made of well-defined spheres (Fig. 4), characteristic of opal-AG. For play-of-color Tecopa opals, the spheres were about 335 nm in diameter and arranged in a highly ordered network, allowing diffraction of light (Fig. 4a and 4b). Opal-AG usually does not present such a remarkable structure on a freshly broken surface (Gaillou et al., 2008b), after etching, as the HF removed the presence of the dense cement. In the case of Tecopa opals, the spheres are loosely packed with little cement (Fig. 4a), causing their porousness. Contact features between the spheres are clearly visible, which is (so far) unique in opals from Tecopa (Ma & Rossman, 2003). Common opal-AG samples from Tecopa have spheres that are large (~700 nm) and not organized, preventing light diffraction (Fig. 5). Little cementation was observed. The spheres were more closely packed than for the play-of-color opals, which gave rise to beehive-like arrangement of the spheres (Fig. 5). In some micrographs after HF etching (Fig. 5), the break went through some spheres, showing that they present a concentric structure in their center, typical of opal-A (Gaillou et al., 2008b).

Characterization of the water in Tecopa opals

Analyzed opals show $\delta^{18}O$-values between 27.6 and 29.5 ‰, while the dehydrated (at 250°C) or melted opals show a consistent $\delta^{18}O$ of 30.5 ‰ (Table 1). The fact that dehydrated and melted opals have the same $\delta^{18}O$ ($\delta^{18}O_{silica}$) indicates that no significant isotopic exchange between water and silica occurred during the water extraction. It also tends to show that both procedure (2 and 3) leads to a complete water removed from opal. Indeed, during partial extraction of water, different isotopic fractionations in the two different dehydration procedures would be expected due to kinetic processes. It is noteworthy that the VBM method (vaccum bead melting) suggested by Chapligin et al. (2010) is similar to the procedure 3 from

this study and generates some isotopic fractionations, which were not observed in our study. This could probably be explained by the fact that during the laser melting, we pump away the extracted water while in the VBM the water is pumped away after, which could lead to isotopic exchange between water and silica during opal metling.

Overall, the $\delta^{18}O$ measured on the dehydrated and melted opals from this study represent the $\delta^{18}O$ of opal silica only. Up to 2 ‰ variation is observed in $\delta^{18}O$-values between opals from the two different nodules analyzed and 1 ‰ difference was measured between the two different opals from the same nodule (opal 1a and opal 1b). However, no significant variation ($\leq$ 0.2 ‰) is observed in the different dehydrated opals, illustrating the oxygen isotopic composition homogeneity of the silica from Tecopa opals. The HRT ash layer that hosts the opal nodules has a $\delta^{18}O$ = 15.8 ± 0.3 ‰ and nodule 1 matrix has $\delta^{18}O$ = 21.4 – 22.4 ‰ (Table 1). Considering the opal composition from the same nodule and by mass balance calculation, we determined that between 43 and 56 % of the nodule1 matrix consists of opal filling small vesicles.

The hydrogen isotopic composition of the opal dehydrated at 34 % is -90 ± 2 ‰ (Table 2), and the dehydrated opal at 40 % and 43 % (2.1 and 2.0 wt.% total water) has a lower δD of -107 ‰ and -101 ‰, respectively. The HRT volcanic ash layer hosting the opals consists of hydrous glass shards, which contain 3.6 ± 0.2 wt.% total water with a δD of -92 ± 5 ‰ (Martin et al., 2017). The water in the ash is meteoritic due to secondary re-hydration of the volcanic glass after its deposit (Taylor, 1968; Friedman et al., 1993b; Martin et al., 2017).

Discussion

Conditions of opal formation:

The consistent $\delta^{18}O_{silica}$ = 30.5 ± 0.1 ‰ measured in different Tecopa opals indicates that they were precipitated from the same fluid under the same temperature conditions. In the

Tecopa basin, the present-day spring waters have $\delta^{18}O$-values between -13 ‰ and -11 ‰ and temperatures typically between 15°C and 30°C, while some spring waters have temperature lower than 10°C and others higher than 40°C (Larsen et al., 2001).

To the best of our knowledge, no studies have discussed the oxygen isotope fractionation coefficient as a function of the temperature between water and silica in gem opals. However, some studies discuss this isotopic fractionation in biogenic opal-A from marine diatoms (e.g. Brandiss et al., 1998; Juillet-Leclerc and Labeyrie, 1987; Schmidt et al., 2001). In diatom opals, in addition to the temperature, some more complex biogenic processes contribute to the isotopic fractionation between silica and water. In terms of isotopic compositions, these biogenic opals are the closest to the opals from this study, compared to quartz that is the most often used for isotopic fractionation experiments between silica and water (e.g. Sharp et al. 2016 for a review). Furthermore, the relation between oxygen isotope fractionation coefficients and temperature from Brandiss et al. (1998) are based on fresh diatoms. Hence biogenic processes play a major role in the isotopic fractionation, which is not the case in gem opal formation as those from Tecopa. However, Juillet-Leclerc and Labeyrie's (1987) result is based on fossil diatoms for which the isotopic composition records the fossilization or silica maturation process conditions as opposed to the initial opal formation during diatom life (e.g. Schmidt et al., 2001). Non-biogenic processes are inferred in this secondary process and this is the reason why we suggest that Juillet-Leclerc and Labeyrie's (1987) fractionation coefficient is more accurate to assess gem opal formation conditions at low temperature (<50°C). Finally and for comparison we will also consider the recent calibration of the SiO_2-H_2O isotopic fractionation for a wide temperature range from Sharp et al. (2016).

The first approach that we discuss here is the estimation of the water $\delta^{18}O$ by considering that the initial water from which opals precipitated had the same temperature as

277 the present-day spring waters from the Tecopa basin (15°C - 30°C). By using the Brandis et
278 al. (1998) fractionation coefficients, the $\delta^{18}O$ of the initial total water was between -3 ‰ and 0
279 ‰, between -9.5‰ and -4‰ considering the Juillet-Leclerc and Labeyrie (1987) or Sharp et
280 al. (2016) coefficients (Table 3). In all cases, the water is isotopically lighter than the water
281 currently flowing through the Tecopa sediment beds (-12 ± 1 ‰) and respectively 60-70 %
282 and 25-50 % of evaporation of the present-day water springs at 15-30°C is required to reach
283 such values (Fig. 6).

284 The second approach consists of estimating the initial water temperature considering
285 that its $\delta^{18}O$ is the same as in the present day Tecopa spring waters (-12 ± 1 ‰). Brandiss et
286 al. (1998) fractionation coefficient gives formation temperatures of Tecopa opals between -25
287 and -30°C. However, temperatures calculated from the Juillet-Leclerc and Labeyrie (1987) or
288 Sharp et al. (2016) fractionation coefficient results in temperatures between +2 and +10°C
289 (Table 3). Such temperatures are lower than the most common water springs from the Tecopa
290 basin. Negative temperatures are unlikely as water would be frozen and thus not able to flow
291 through sediment beds and precipitate opal. However, +2 to +10°C initial water is more likely
292 and corresponds to the temperature of cold spring waters that are currently present in the
293 Tecopa basin (Larsen et al., 2001).

294 Therefore, we can conclude that Tecopa opals were formed between +2 to +10°C in
295 water having a $\delta^{18}O$ of -12 ± 1 ‰ or at 15-30°C in water having a $\delta^{18}O$ between -9.5 and -4
296 ‰ and as a result undertook 25-50 % evaporation (Fig. 6).

297 Tecopa opals from this study were found in the 2.1 Ma HRT ash layer that is in the K-
298 feldspar diagenetic facies. Now, we can address the question, is the opal formation related to
299 the diagenetic event? The diagenetic zeolite species and K-feldspars observed in the Tecopa
300 basin occur at temperatures higher than 60-70°C (e.g. Larsen, 2008; Utada, 2001). As inferred
301 above, the maximum opal formation temperature is around 30°C, which is still lower than

zeolite and K-feldspar diagenetic facies temperature conditions. Tecopa opals were most likely formed after the diagenetic event as they are opal-A and did not get transformed into opal-CT (e.g. Jones & Segnit, 1971; Jones & Renaut, 2007). This diagenetic event is not well constrained in time (Larsen, 2008; Sheppard and Gude, 1968).

Comparatively with other oxygen isotopic studies on opals in diverse geological settings, this work relates well with the study of Rondeau et al. (2004) on Slovakian gem opals. Indeed, Slovakian opal-AG formed in a volcanic setting, at low temperature (lower than 45°C) with a $\delta^{18}O_{silica}$ of about 31 ‰. In that case and at Lake Tecopa, opal formation was an epigenic process, which happened after the volcanic event. It contrasts with the formation of opal-CT ($\delta^{18}O$ ~ 13 ‰) at higher temperature (~ 160°C) in ignimbrite and in void space in rhyolitic rocks (Rondeau et al., 2004). As previously proposed by Rondeau et al. (2004), this study confirms that the difference between the formation of opal-AG and opal-CT depends (at least) on the temperature of formation: low for opal-AG (so far lower than 45°C) and higher for opal-CT (160°C or higher; Spencer et al., 1992; Rondeau et al., 2004).

Water in opals:

The heterogeneity observed in $\delta^{18}O$ measured in opals (non-dehydrated; $SiO_2 . nH_2O$) shows that water in opals have a different content and/or have heterogeneous composition. We attempted to assess the water $\delta^{18}O$ ($\delta^{18}O_{water}$) by considering the total water content of opals and the opal $\delta^{18}O$ before and after dehydration, Equation 1.

Equation 1: $$\delta O_{water} = \frac{\delta O_{opal} - (1 - 1.68\ X)\,\delta O_{silica}}{1.68\,X}$$

$\delta^{18}O_{opal}$ and $\delta^{18}O_{silica}$ are respectively the values measured for opal before and after dehydration.

X corresponds to the total water wt.% measured and the factor 1.68 corresponds to the enrichment of oxygen in total water relatively to silica. Indeed, O weight is 89wt.% in H_2O, 94wt.% in OH 94% and 53 wt.% in SiO_2. Considering that OH is usually around 10-15% of total water in opal A (e.g. Day and Jones 2008; Langer and

Flörke, 1974), the enrichment is fixed here at 1.68. It is noteworthy that the change between 1.67 (pure H_2O) and 1.68 (85% H_2O and 15%OH) on the $\delta^{18}O_{water}$ calculated is lower than the $\delta^{18}O$ reproducibility on our samples (± 0.1 ‰).

We performed this calculation for the opal 2 from nodule 2 (Table 1) where analyses before and after dehydration have been conducted and where the total water content was measured on the same opal 2 (3.5 wt.%; Table 2). The calculated composition shows a mean value of ~12 ‰ (Table 1 and Fig. 5), which is ~24 ‰ heavier than the actual water composition from the Tecopa basin (-12‰; Fig. 6). Note that the opals (1a and 1b) from nodule 1 show lower $\delta^{18}O$ than the opal from nodule 2, which is consistent with higher total water content measured (4 wt.%). Considering this 4 wt.%, total water $\delta^{18}O$ is between -11.5 ‰ and 6.5 ‰, which is intermediate between the actual water from the Tecopa basin (-12‰) and the isotopically heaviest water calculated from nodule 2 (+12 ‰; Fig. 6). Furthermore, during the melting of opal 2 from nodule 2 (see procedure 3 in the analytical technique section above), the extracted water was trapped in a cold trap, and after fluorination we were able to measure a $\delta^{18}O_{water}$ of 8.5 ‰. It is important to note that the analytical error is high (probably up to 1 or 2 ‰) on this analysis due to the very small amount (2 µmol) of water analyzed. Unfortunately, we did not have enough opal left to repeat the analysis on larger amount of extracted water. Nevertheless, this value is in the same range (according to the analytical errors) as the calculated $\delta^{18}O_{water}$ (~12 ‰) from the same opal and surprisingly drastically different from the actual $\delta^{18}O_{water} \approx$ -12 ‰ from the Tecopa basin (Table 1 and Fig. 6).

The opal formation by precipitation of silica requires an evaporation of the residual water before the opal "consolidation". Such evaporation could explain the relatively high $\delta^{18}O$ measured in opal water compared to the Tecopa groundwater. Using the isotopic fractionation from Horita and Wesolowski (1994), we estimate that 80-95 % of evaporation at 5-30°C is

352 required in order to increase the $\delta^{18}O$ of the initial water (-12 ‰) up to ~12 ‰ (Fig. 6).
353 Finally, figure 6 shows that opal can record the water composition during different stages of
354 its formation and specifically the latest ones (from 15 % to 95 % water evaporation).

355 The analysis of hydrogen isotopes in opal shows a direct link to the water composition.
356 In this study, δD of -90 ± 2 ‰ was measured in 34 % dehydrated opals. The actual water that
357 is present in the Tecopa basin is δD = -100 ‰ to -95 ‰ (Larsen et al., 2001), thus the total
358 water contained in Tecopa opals has apparently a comparable composition than the
359 isotopically heaviest water from the Tecopa basin. Hydrogen isotope ratio of the HRT
360 volcanic ash layer that hosts opals is -92 ±5 ‰, which is comparable to what is measured in
361 opals. Considering a comparable isotopic fractionation between water - amorphous silicic
362 glass and water – opal at relatively low temperature (5-30°C) and knowing that the origin of
363 water from the volcanic ash is secondary due to re-hydration of the glass (Taylor 1968;
364 Friedman 1993, Martin et al. 2017), the water from which the opal precipitated had a
365 relatively similar composition to the water that re-hydrated the volcanic silicic glass. The HRT
366 ash deposit is 2.1 Ma, and considering that glass hydration took place soon after its deposit,
367 the water composition in the Tecopa basin today seems relatively similar to the water in the
368 same basin 2.1Ma ago.

369 The fractionation coefficient of the D/H ratio between water and opal is not known, but
370 it is strongly dependent on the ratio between the molecular (H_2O_m) and structural (OH) water
371 as well known in amorphous silicic glass (e.g. Dobson et al., 1989; Newman et al., 1988;
372 Pineau et al., 1998). In opal, OH corresponds to water bounded to silica, whereas H_2O_m is
373 most likely adsorbed on the surface and fills the pores (Langer and Florke, 1974, Flörke et al.,
374 1991). In opal-A, due to its compact structure, the proportion of OH is usually about 10-15 %
375 of the total water, while in opal-CT, OH is about 3-4 % of the total water (e.g. Day and Jones
376 2008; Langer and Flörke, 1974)

In nodule 2, opals dehydrated at 34 % have a δD of -90‰, while a δD of about -104 ‰ is measured in opals dehydrated at 40-43% (table 2). During dehydration at 110°C, molecular H_2O_m is easily removed from opal while OH stays most likely bounded to the opal silica (e.g. Thomas et al. 2007). Therefore the fact the δD decreases with dehydration shows that H_2O_m is isotopically heavier (higher δD) than OH. This is similar to what is observed in silicic magmas, where δD of H_2O_m is expected to be ~65 ‰ higher than in OH (De Hoog et al., 2009, and references therein).

Implications

This study shows that in the Tecopa basin, opals were formed between 2 and 30°C, from water circulating in the host volcanic ash bed (2-10°C from the basin groundwater similar to present conditions or at 15-30°C after 25-50% evaporation of this groundwater). On the other hand, oxygen isotope composition of opal's water indicates different stages of opal formation from groundwater. Opal seems to precipitate from groundwater that is experiencing isotopic distillation during its circulation, most likely due to an evaporation mechanism, from 15 % up to 80-95 %. Finally, hydrogen isotopic analysis show that molecular water (H_2O_m) is isotopically heavier that structural water (OH).

Further work must be done in order to determinate the O- and H-isotopic composition and speciation of water in opals from other localities and from other types (opal-CT, opal-C). Indeed, this kind of approach on amorphous silica materials such as volcanic glass and cherts are widely used to discuss paleoclimate or paleoenvironment reconstitutions (e.g. Taylor, 1968; Friedman et al., 1993b; Hren et al., 2009; Marin-Carbonne et al., 2014; Mulch et al., 2008; Pingel et al., 2014; Saylor and Horton, 2014; Martin et al. 2017).

As paleoenvironments go, studies are not limited to Earth. On Mars, at Gale and Gusev craters, diagenetic silica enrichment was observed in bedrock layers (Squyres et al., 2008;

Ruff et al., 2011; Ruff and Farmer, 2016; Frydenvang et al., 2017, Hurowitz et al., 2017). This enrichment might have come as a later process of mobilization of surrounding silica-rich volcanic rocks at lower temperatures than previously thought (Frydenvang et al., 2017). Tecopa opals from this study could be a better analog for silica enriched zones on Mars, with water mobilization at low temperature, and where opal-A might thrive.

Acknowledgment

The authors are thankful to Jeffrey Post and Tim Rose from the Smithsonian Institution for their help with the SEM and X-ray diffraction analyses. We are grateful to Ilya Bindeman for letting us using his lab at the University of Oregon and Marli Miller and Darrel Cowan for their accommodation at Shoshone during the field work. We would like to express the deepest appreciation to Alyssa Morgan, from the Natural History Museum of Los Angeles County, for proof-reading this manuscript. Finally, the authors thank G. R. Rossman, A, Celestian and the anonymous reviewers for their constructive comments that improved the manuscript.

REFERENCES

Brandiss, M.E., O'Neil, J.R., Edlund, M.B., and Stoermer, E.F. (1998) Oxygen isotope fractionation between diatomaceous silica and water. Geochimica et Cosmochimica Acta, 62, 1119-1125.

Campbell, K.A., Guido, D.M., Gautret, P., Foucher, F., Ramboz, C., Westall, F. (2015) Geyserite in hot-spring siliceous sinter: Window on Earth's hottest terrestrial (paleo)environment and its extreme life. Earth Science Reviews, 148, 44-64.

Chapligin, B., Meyer, H., Friedrichsen, H., Marent, A.,Sohns E. and Hubberten H.-W. (2010) A high-performance, safer and semi-automated approach for the δ 18O analysis of diatom silica and new methods for removing exchangeable oxygen. Rapid Communications in Mass Spectrometry, 24, 2655-2664.

Chauviré, B., Rondeau, B., Mangold, N. (2017) Near infrared signature of opal and chalcedony as a proxy for their structure and formation conditions. European Journal of Mineralogy, 29, 409-421.

Crowley J.L., Schoene, B., Bowring S.A. (2007) U-Pb dating of zircon in the Bishop Tuff at the millennial scale. Geology, 35, 1123-1126.

Day, R., and Jones, B. (2008) Variations in Water Content in Opal-A and Opal-CT from Geyser Discharge Aprons. Journal of Sedimentary Research, 78, 4, 301-315.

De Hoog, J.C.M., Taylor, B.E., and Van Bergen, M.J. (2009) Hydrogen-isotope systematics in degassing basaltic magma and application to Indonesian arc basalts. Chemical Geology, 266(3–4), 256-266.

De La Rocha, C. L. , Brzezinski, M. A., DeNiro, M. J., and Shemesh, A. (1998) Silicon-isotope composition of diatoms as an indicator of past oceanic change. Nature, 395, 680-683.

Des Cloizeaux, A., 1862. In: Dunod (Ed.), Manuel de Minéralogie. Paris. 572 pp.

Dobson, P.F., Epstein, S., and Stolper, and E.M. (1989) Hydrogen isotope fractionation between coexisting vapor and silicate glasses and melts at low pressure. Geochimica et Cosmochimica Acta, 53, 10, 2723-2730.

Flörke O.W., Graetsch H., Martin B. Röller K. and Wirth R. (1991) Nomenclature of micro and non-crystalline silica minerals, based on structure and microstructure. Neues Jahrbuch für Mineralogie Monatshefte, 163, 19-42.

Friedman, I., Gleason, J., Sheppard, R.A., and Gude, A.J. (1993a) Deuterium fractionation as water diffuses into silicic volcanic ash. AGU, Geophysical monograph, 78, 321-323.

Friedman, I., Gleason, J., and Warden, A. (1993b) Ancient climate from deuterium content of water in volcanic glass. AGU, Geophysical monograph, 78, 309-319.

Fritsch E., Rondeau B., Ostrooumov M., Lasnier B., Marie A.M., Barrault A., Wery J., Connoué J., and Lefrant S. (1999) Découvertes récentes sur l'opale. Revue de Gemmologie a.f.g., 138/139, 34-40.

Frydenvang, J., Gasda, P. J., Hurowitz, J.A., Grotzinger, J.P., Wiens, R.C., Newsom, H.E., Edgett, K.S., Watkins, J., Bridges, J.C., Maurice, S., Fisk, M.R., Johnson, J.R., Rapin, W., Stein, N.T., Clegg, S.M., Schwenzer, S.P., Bedford, C.C., Edwards, P., Mangold, N., Cousin, A., Anderson, R.B., Payré, V., Vaniman, D., Blake D. F. , Lanza, N. L., Gupta, S., Van Beek, J., Sautter V., Meslin P.-Y., Rice M., Milliken, R., Gellert, R., Thompson, L., Clark B.C., Sumner, D.Y., Fraeman, A.A., Kinch, K.M., Madsen, M.B., Mitrofanov, I.G., Jun, I., Calef, F., and Vasavada, A. R. (2017) Diagenetic silica enrichment and late-stage groundwater activity in Gale crater, Mars. Geophysical Research Letters, 44, 4716-4724.

Gaillou, E., Delaunay, A., Rondeau, B., Bouhnik-le-Coz, M., Fritsch, E., Cornen, G. and Monnier, C. (2008a) The geochemistry of gem opals as evidence of their origin. Ore Geology Reviews, 34, 113–126.

Gaillou, E., Fritsch, E., Aguilar-Reyes, B., Rondeau, B., Post, J.E., Barreau, and A., Ostroumov, M. (2008b) Common gem opal: An investigation of micro- to nano-structure. American Mineralogist, 93, 1865–1873.

Gübelin, E. (1986) Les opales mexicaines. Revue de Gemmologie a.f.g., 88, 3-8.

Hillhouse, J.W. (1987) Late Tertiary and Quaternary geology of the Tecopa basin, southeastern California. Miscellaneous Investigations Series - U. S. Geological Survey

Holzhey, G. (1997) Feueropal von Opal Butte, Oregon, USA. Zeitung Deutsche Gemmologische Gesellschaft, 46, 3,161-167.

Horita, J., and Wesolowski, D.J. (1994) Liquid-vapor fractionation of oxygen and hydrogen isotopes of water from the freezing to the critical temperature. Geochimica et Cosmochimica Acta, 58(16), 3425-3437.

Hren, M.T., Tice, M.M., and Chamberlain, C.P. (2009) Oxygen and hydrogen isotope evidence for a temperate climate 3.42 billion years ago. Nature, 462(7270), 205-208.

Hurowitz, J. A., S. M. McLennan, N. J. Tosca, R. E. Arvidson, J. R. Michalski, D. W. Ming, C. Schröder, and S. W. Squyres (2006) In situ and experimental evidence for acidic weathering of rocks and soils on Mars. Journal of Geophysical Research, 111, E02S19.

Jones, J.B., and Segnit, E.R., 1971. The nature of opal. Part 1: Nomenclature and constituent phases. Journal of the Geological Society of Australia, 8, 57-68.

Jones, B., Renaut, R.W. (2007) Microstructural changes accompanying the opal-A to opal-CT transition: new evidence from the siliceous sinters of Geysir, Haukadalur, Iceland. Sedimentology, 54, 921-948.

Jones, J.B., Sanders, J.V. and Segnit, E.R. (1964) Structure of opal. Nature, 204, 4962, 990-991.

Juillet-Leclerc, A., and Labeyrie, L. (1987) Temperature dependence of the oxygen isotopic fractionation between diatom silica and water. Earth and Planetary Science Letters, 84, 69-74.

Kakiuchi, M., and Matsuo, S. (1979) Direct measurements of D/H and $^{18}O/^{16}O$ fractionation factors between vapor and liquid water in the temperature range from 10 to 40°C. Geochemical Journal, 13, 307-311.

501 Koivula, J.I., Fryer, C.W., and Keller, C.P. (1983) Opal from Queretaro, occurrence and
502 inclusions. Gems and Gemology, 19, 2, 87-98.
503 Lacroix, A.,(1896) Minéralogie de la France. 1962 reprint, A. Blanchard, Ed., Paris. vol. II, p.
504 446 and vol. III, p. 316–337.
505 Langer K. and Flörke O.W. (1974) Near infrared absorption spectra (4000-9000 cm-1) of
506 opals and the role of « water » in these SiO_2 .n H_2O minerals. Fortschitte der
507 Mineralogie, 52, 17-51.
508 Larsen, D. (2008) Revisiting silicate authigenesis in the Pliocene-Pleistocene Lake Tecopa
509 beds, southeastern California: Depositional and hydrological controls. Geosphere, 4,
510 612-639.
511 Larsen, D., Swihart, G.H., and Xiao, Y. (2001) Hydrochemistry and isotope composition of
512 springs in the Tecopa basin, southeastern California, USA. Chemical Geology, 179,
513 17–35.
514 Ma, C., and Rossman, G.R. (2003) Low voltage FESEM of geological materials. Microsc.
515 Microanal., 9, 990-991.
516 Marin-Carbonne, J., Robert, F., and Chaussidon, M. (2014) The silicon and oxygen isotope
517 compositions of Precambrian cherts: A record of oceanic paleo-temperatures?
518 Precambrian Research, 247, 223-234.
519 Martin, E., and Bindeman, I. (2009) Mass-independent isotopic signatures of volcanic sulfate
520 from three supereruption ash deposits in Lake Tecopa, California. Earth and Planetary
521 Science Letters, 282, 102-114.
522 Martin, E., Bindeman, I.N., Balan, E., Palandri, J., Seligman, A., and Villemant, B. (2017)
523 Hydrogen isotope determination by TC/EA technique in application to volcanic glass
524 as a window into secondary hydration. Journal of Volcanology and Geothermal
525 Research, 348, 49-61.

526 Matthews N.E., Vazquez J.A. and Calvert, A. (2015) Age of the Lava Creek supereruption and
527 magma chamber assembly at Yellowstone based on $^{40}Ar/^{39}Ar$ and U-Pb dating of
528 sanidine and zircon crystals. Geochemistry, Geophysics, Geosystems, 16, 2508-2528.
529 Morrison, R.B. (1999) Lake Tecopa: Quaternary geology of Tecopa Valley, California, a
530 multimillion-year record and its relevance to the proposed nuclear-waste repository at
531 Yucca Mountain, Nevada. In L.A. Wright, and B.W. Troxel, Eds. Cenozoic Basins of
532 the Death Valley Region: Boulder, Colorado, Special paper 333. Geological Society of
533 Amercia.
534 Mulch, A., Sarna-Wojcicki, A.M., Perkins, M.E., and Chamberlain, C.P. (2008) A Miocene to
535 Pleistocene climate and elevation record of the Sierra Nevada (California).
536 Proceedings of the National Academy of Sciences, 105, 6819-6824.
537 Newman, S., Epstein, S., and Stolper, E. (1988) Water, carbon dioxide, and hydrogen isotopes
538 in glasses from the ca. 1340 A.D. eruption of the Mono Craters, California:
539 Constraints on degassing phenomena and initial volatile content. Journal of
540 Volcanology and Geothermal Research, 35(1–2), 75-96.
541 Ostrooumov, M., Fritsch, E., Lasnier, B., and Lefrant, S. (1999) Spectres Raman des opales:
542 Aspect diagnostique et aide à la classification. European Journal of Mineralogy, 11,
543 899–908.
544 Payette, F. (1999) A propos de l'opale australienne. Revue de Gemmologie a.f.g. 138–139,
545 67–71.
546 Pineau, F., Shilobreeva, S., Kadik, A., and Javoy, M. (1998) Water solubility and D/H
547 fractionation in the system basaltic andesite–H_2O at 1250°C and between 0.5 and 3
548 kbars. Chemical Geology, 147(1–2), 173-184.

549 Pingel, H., Alonso, R.N., Mulch, A., Rohrmann, A., Sudo, M., and Strecker, M.R. (2014)
550 Pliocene orographic barrier uplift in the southern Central Andes. Geology, 42(8), 691-
551 694.
552 Rey, P.F. (2013) Opalisation of the Great Artesian Basin (central Australia): an Australian
553 story with a Martian twist. Australian Journal of Earth Sciences, 60, 3, 291-314.
554 Rivera, T.A., Schmitz, M. D., Crowel, J.L. and Storey M. (2014) Rapid magma evolution
555 constrained by zircon petrochronology and $^{40}Ar/^{39}Ar$ sanidine ages for the
556 Huckleberry Ridge Tuff, Yellowstone, USA. Geology, 42, 643-646.
557 Rondeau, B., Fritsch, E., Guiraud, M., and Renac, C. (2004) Opals from Slovakia
558 ("Hungarian" opals) - a re-assessment of the conditions of formation. European
559 Journal of Mineralogy, 16, 789-799.
560 Rondeau, B., Cenki-Tok, B., Fritsch, E., Mazzero, F., Gauthier, J.-P., Bodeur, Y, Bekele, E.,
561 Gaillou, E., and Ayalew, D. (2012) Geochemical and petrological characterization of
562 gem opals from Wegel Tena, Wollo, Ethiopia: opal formation in an Oligocene soil.
563 Geochemistry: Exploration, Environment, Analysis, 12, 93-104.
564 Ruff, S.W., and J.D. Farmer (2016) Silica deposits on Mars with features resembling hot
565 spring biosignatures at El Tatio in Chile. Nature Communications, 7, 13, 554.
566 Ruff, S.W., Farmer J.D., Calvin, W.M., Herkenhoff, K.E., Johnson J.R., Morris, R.V, Rice
567 M.S., Arvidson R.E., Bell III, J.F, Christensen, P.R., and Squyres, S.W (2011)
568 Characteristics, distribution, origin, and significance of opaline silica observed by the
569 Spirit rover in Gusev crater, Mars. Journal of Geophysical Research, 116, E00F23, 1-
570 48.
571 Saylor, J.E., and Horton, B.K. (2014) Nonuniform surface uplift of the Andean plateau
572 revealed by deuterium isotopes in Miocene volcanic glass from southern Peru. Earth
573 and Planetary Science Letters, 387(0), 120-131.

574 Schmidt, M., Botz, R., Rickert, D., Bohrmann, G., Hall, S.R., and Mann, S. (2001) Oxygen
575 isotopes of marine diatoms and relations to Opal-A maturation. Geochimica et
576 Cosmochimica Acta, 65, 201-211.
577 Sharp Z.D., Gibbons, J.A., Maltsev, O., Atudorei, V., Pack, A., Sengupa, S., Shock, E.L. and
578 Knuauth, L.P. (2016) A calibration of the triple oxygen isotope fractionation in the
579 SiO2-H2O system and applications to natural samples. Geochimica et Cosmichimica
580 Acta, 186, 105-119.
581 Sheppard, R.A., and Gude, A.J. (1968) Distribution and genesis of authigenic silicate minerals
582 in tuffs of Pleistocene Lake Tecopa, Inyo County, California. United State Geological
583 Survey Professional Paper, 597, 38p.
584 Smallwood, A.G. (2000) A preliminary investigation of precious opal by laser Raman
585 spectroscopy. The Australian Gemmologist, 20, 9, 363-366.
586 Smallwood, A.G., Thomas, P.S. and Ray, A.S. (1997) Characterisation of sedimentary opals by
587 Fourier Transform Raman spectroscopy. Spectrochimica Acta, Part A, 53, 2341-2345.
588 Smallwood, A.G., Thomas, P.S. and Ray, A.S. (2008) Comparative Analysis of Sedimentary
589 and Volcanic Precious Opals from Australia. Journal of the Australian Ceramic Society
590 Volume 44[2], 17-22.
591 Spencer, R.J., Levinson, A.A., and Koivula, J.I. (1992) Opal from Querétaro, Mexico: Fluid
592 inclusions study. Gems and Gemology, 28, 1, 28-34.
593 Squyres, S.W., Arvidson, R.E., Ruff, S., Gellert, R., Morris, R.V., Ming, D.W., Crumpler, L.,
594 Farmer, J. D., Des Marais, D. J., Yen, A., McLennan, S. M., Calvin, W., Bell III, J. F.,
595 Clark, B.C., Wang, A., McCoy, T.J., Schmidt, M.E., and de Souza Jr., P.A. (2008)
596 Detection of silica-rich deposits on Mars. Science, 320 (5879), 1063–1067.
597 Strakey, H.C., Blackmon, P.D., (1979) Clay mineralogy of Pleistocene Lake Tecopa, Inyo
598 County, California. United State Geological Survey Professional Paper, 1061: 34p.

599 Taylor, H.P. (1968) The oxygen isotope geochemistry of igneous rocks. Contribution ot
600 Mineralogy and Petrology, 1-71.
601 Thomas, P.S., Simon, P., Smallwood, A.S., and Ray, A.S. (2007) Estimation of the diffusion
602 coefficient of water evolved during the non-isothermal dehydration of Australian
603 sedimentary opal. Journal of Thermal Analysis and Calorimetry, 88, 231-235.
604 Utada, M., (2001) Zeolites in hydrothermally altered rocks. Reviews in mineralogy and
605 geochemistry, 45, 305-322.
606 Webster, R. (1975) Opal. Gems, their sources, description and identification, revised par B.W.
607 Anderson, 3rd edition, Butterworths, London. pp. 199-209.
608
609
610

Figure Captions:

Figure 1 :

Map of the southwest of the United States of America, showing the location of the Tecopa basin, southeast of Death Valley.

Figure 2 :

Photos of Tecopa opals on the field: A) Small valley where gem opals from this study were collected. The HRT ash layer is highlighted by white dotted lines; B) Close-up on the HRT ash layer that hosts the gem opals; C) One of the nodules present in the ash layer that contains opals; D) siliceous clay nodules in the HRT tuff bed; E) Opal in the interior of a nodule (note the hand lenses for scale); F) Play-of-colors in some opals.

Figure 3: Diffractogram of play-of-color opal 5, showing mostly an amorphous band at 4.1 Å, typical of opal-A. Diffractogram of the common opal 4 showed a similar pattern.

Figure 4: SEM picture of a Tecopa play-of-color opal-AG on a freshly broken surface. A) In Opal 5, the perfect stacking of spheres ~ 330 nm in diameter is visible, as well as the loose cement in between spheres' layers. B) After HF etching of Opal 5, most of the cement is removed, revealing a perfectly packed structure. Contact features between the spheres are characteristic of Tecopa opals.

Figure 5: SEM picture of Tecopa common Opal 4 on a freshly broken surface. The spheres are too big (~700 nm) and not well-packed, precluding light diffraction, thus play-of-color. Notice the internal concentric structure.

Figure 6: Oxygen isotope composition of opal silica as well as of the water from which it precipitates during evaporation at 5°C and 30°C. Initial water composition is from Larsen (2001), isotopic fractionations of water during evaporation are from Horita and Wesolowski (1994) and isotopic fractionations between opal silica and water are from Juillet-Leclerc and Labeyrie (1987) and Sharp et al. (2016). Values reported in the figure (measured or calculated) are the mean values from the table 1 and are discussed in details in the text.

This is a preprint, the final version is subject to change, of the American Mineralogist (MSA)
Cite as Authors (Year) Title. American Mineralogist, in press.
DOI: https://doi.org/10.2138/am-2018-6131

Table 1 : **Oxygen isotope compositions of opals and host rocks.** *Different* $\delta^{18}O$ *values for the same sample correspond to replicates.*

		$\delta^{18}O$ (‰)	mean $\delta^{18}O$ (‰)	calculated water $\delta^{18}O$ (‰) *	
Nodule 1	opal 1a	27.3	27.6	-11.3 *(±5.8)*	
		27.8			
		27.8			
	opal 1b	28.8	28.8	6.6 *(±2.8)*	
	opal 1a + 1b *dehydrated*	30.2	30.4		
		30.6			
		30.4			
Nodule 2	opal 2	29.2	29.5	11.9 *(±6.5)*	
		29.8			
	opal 2 *dehydrated*	30.5	30.6		
		30.6			
	opal 2 *melted*	30.5	30.5	8.5**	
		30.5			
Ash deposit		15.5	15.8		
		16.1		opal proportion (%)	
Nodule 3 (clay + opal)		21.4		(1) 47	(2) 43
		22.4		(1) 56	(2) 52

* *Equation 1:* $$\delta O_{water} = \frac{\delta O_{opal} - (1 - 1.68\,X)\delta O_{silica}}{1.68\,X}$$

$\delta^{18}O_{opal}$ and $\delta^{18}O_{silica}$ are respectively the mean values measured for opal before and after dehydration. *X corresponds to the total water wt.% measured and the factor 1.68 corresponds to the enrichment of oxygen in total water relatively to silica. Indeed, O weight is 89wt.% in H_2O, 94wt.%, in OH 94% and 53 wt.% in SiO_2. Considering that OH is usually around 10-15% of total water in opal A (e.g. Day and Jones 2008; Langer and Flörke, 1974), the enrichment is fixed here at 1.68. It is noteworthy that the change between 1.67 (pure H_2O) and 1.68 (85% H_2O and 15%OH) on the $\delta^{18}O_{water}$ calculated is lower than the $\delta^{18}O$ reproducibility on our samples (± 0.1 ‰).*

** *Value measured in water extracted from opal during the opal melting (see text for details).*

This is a preprint, the final version is subject to change, of the American Mineralogist (MSA)
Cite as Authors (Year) Title. American Mineralogist, in press.
DOI: https://doi.org/10.2138/am-2018-6131

Table 2: Total Water content and hydrogen isotope compositions of opal and host rock. *Different δD and total water content values for the same sample correspond to replicates.*

		Total water content (wt.%)	% of dehydration	δD	mean δD
Nodule 1	opal 1c	4.0*	-	-	-
Nodule 2	opal 2	3.5*	0%	-	-
	opal 2**	2.3	34%	-87	-90
		2.3		-90	
		2.3		-92	
	opal 2***	2.0	43%	-101	-104
		2.1	40%	-107	
Host rock	Volcanic ash	3.7		-89	-92
		3.5		-95	

** Total water content measured by mass difference of the opal before and after 3 hours in a vacuum oven at 250°C.*

*** 34% dehydration was obtained by letting the opal in a desiccator for a few days.*

****40-43% dehydration was obtained after 2 hours in a vacuum oven at 110°C.*

Table 3 : Water composition and temperature from which opal precipitated.

	Initial $\delta^{18}O_{water}$	Initial water T°C
Brandiss et al. (1998)	-13‰ to -11‰	**-20 to -30°C**
	-3‰ to 0‰	15 to 30°C
Juillet-Leclerc and Labeyrie, (1987)	-13‰ to -11‰	**5 to 10°C**
	-9.5‰ to -5.5‰	15 to 30°C
Sharp et al. (2016)	-13‰ to -11‰	**2 to 8°C**
	-9‰ to -4‰	15 to 30°C

Brandiss et al. (1998): $1000Ln\alpha = 15.56.10^3/T - 20.92$, Juillet-Leclerc and Labeyrie (1987) $1000Ln\alpha = 3.26.10^6/T^2 + 0.45$ and Sharpet al. (2016) : $1000Ln\alpha = 4.2.10^6/T^2 - 3.3.10^3/T$ (α : oxygen isotopes fractionation coefficient between silica and water; T: temperature). Values in bold are calculated values and the others are fixed values from the present-day Tecopa spring waters (Larsen et al., 2001).


Oregon
Idaho
Nevada
California
Arizona
San Francisco
Death
valley
Las Vegas
Tecopa
Los Angeles
Pacific Ocean
Mexico


A


B
1m


C


D

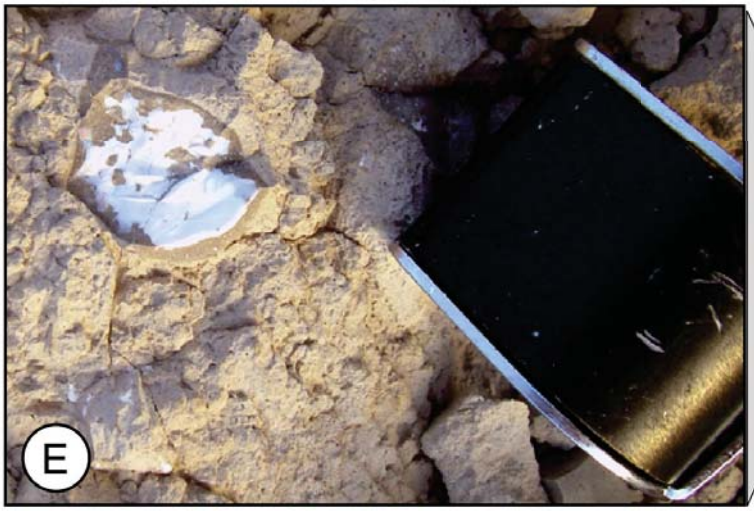
E

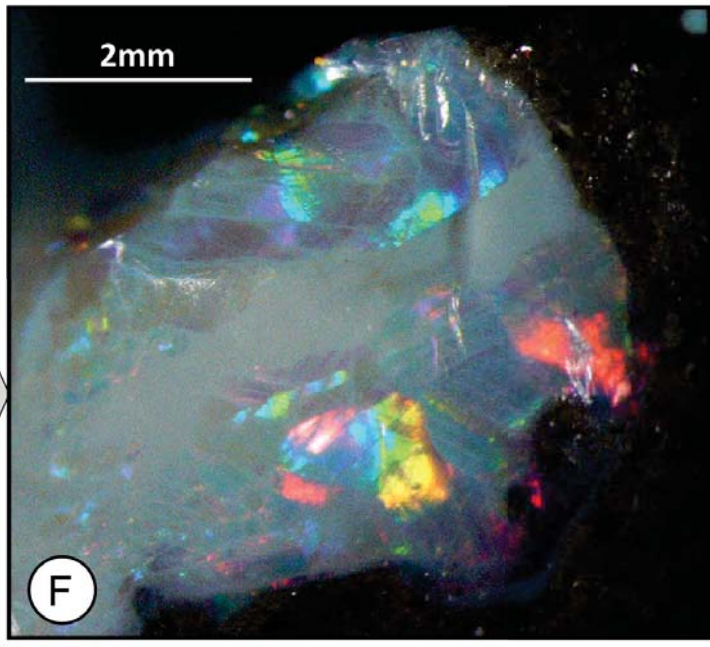
2mm
F

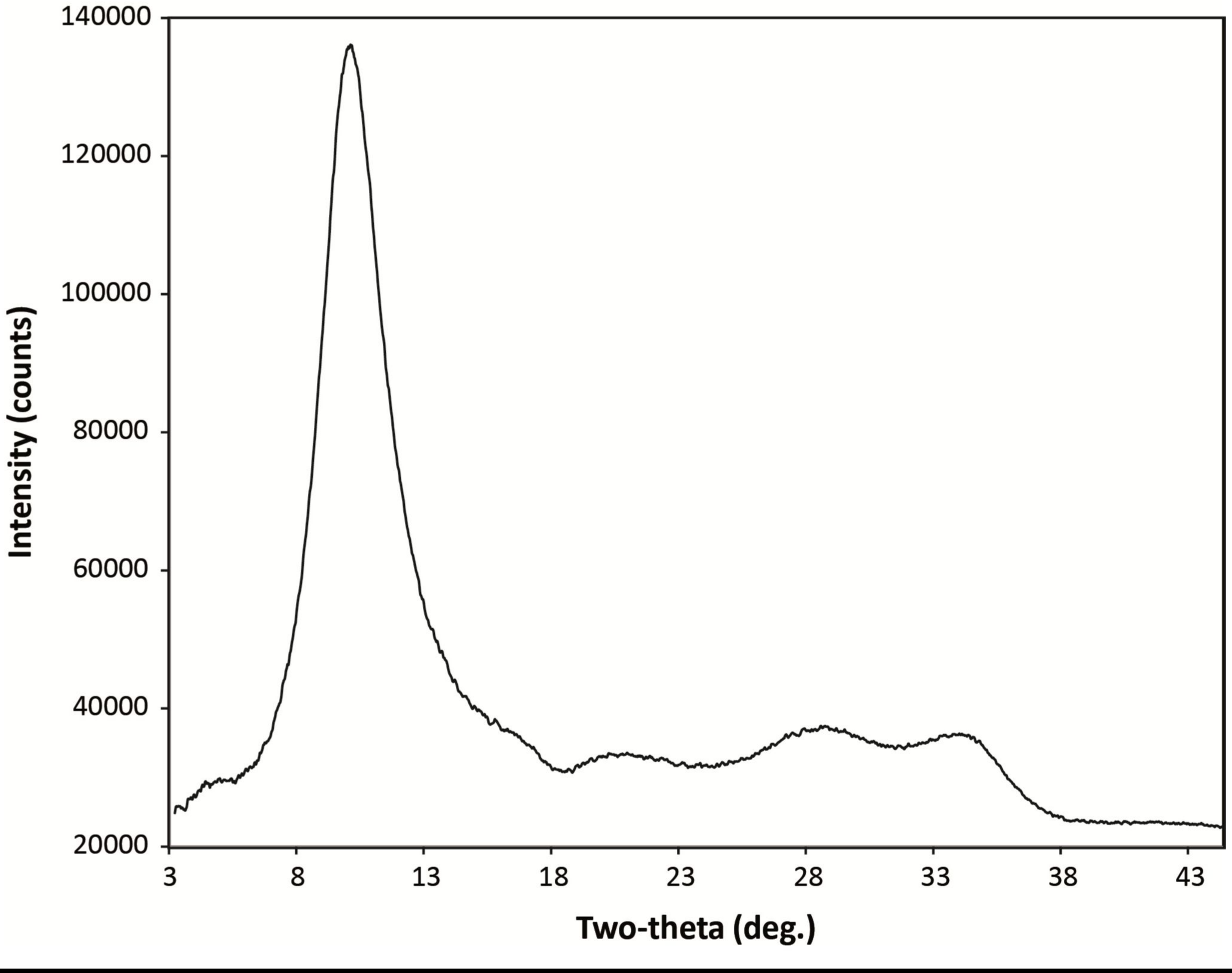
140000
120000
100000
80000
60000
40000
20000
Intensity (counts)
3
8
13
18
23
28
33
38
43
Two-theta (deg.)

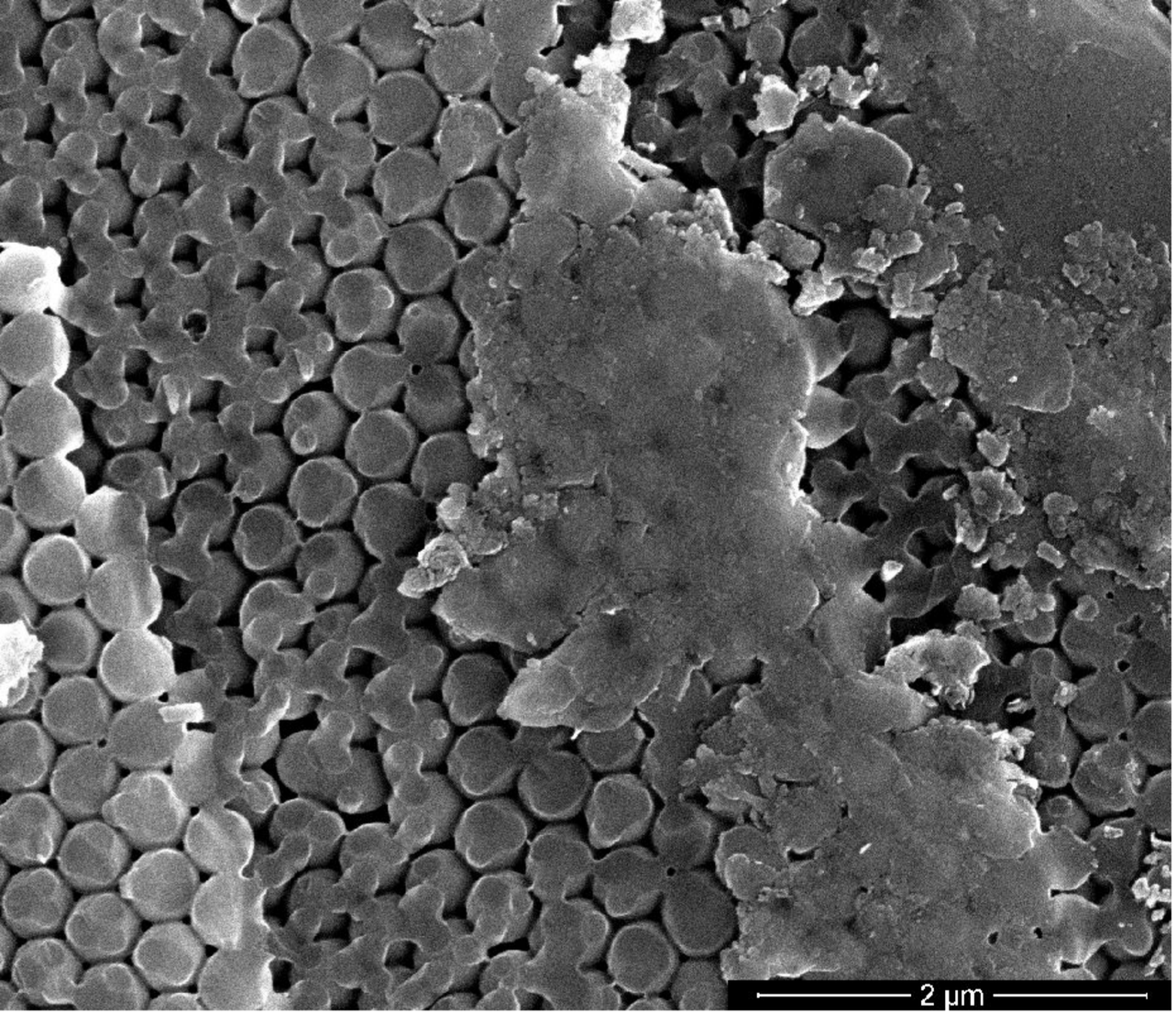
2 µm

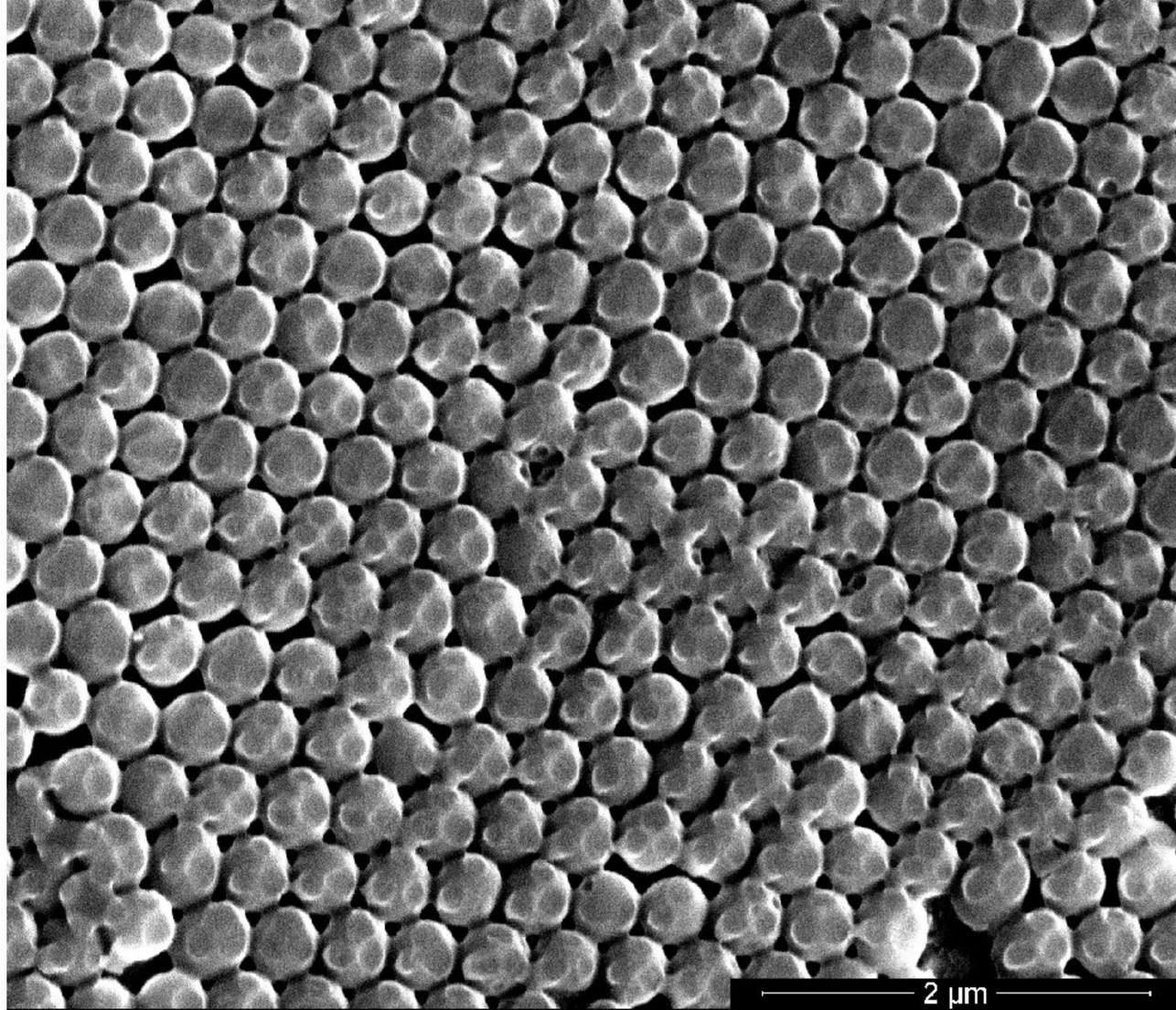
2 µm

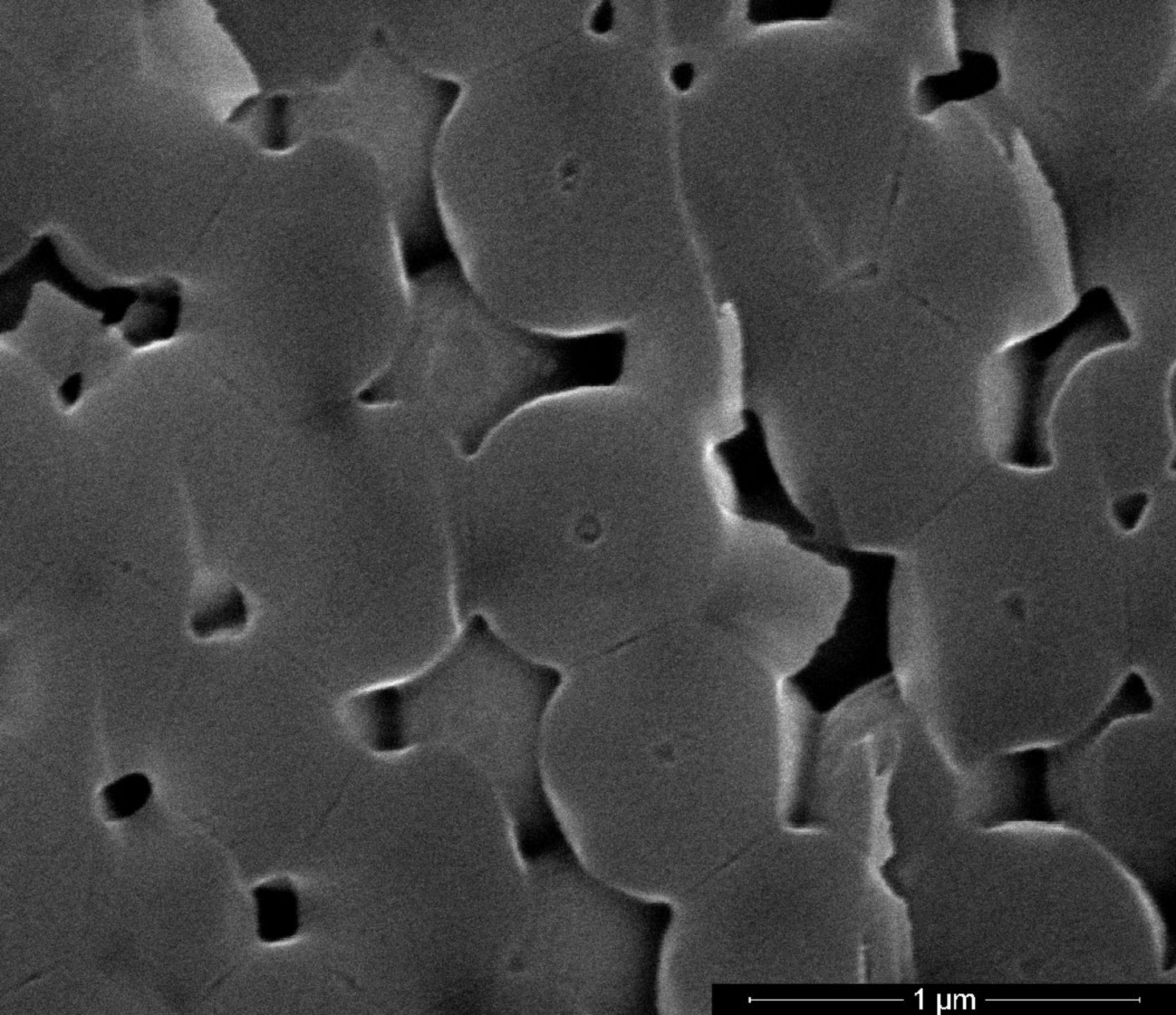
1 µm

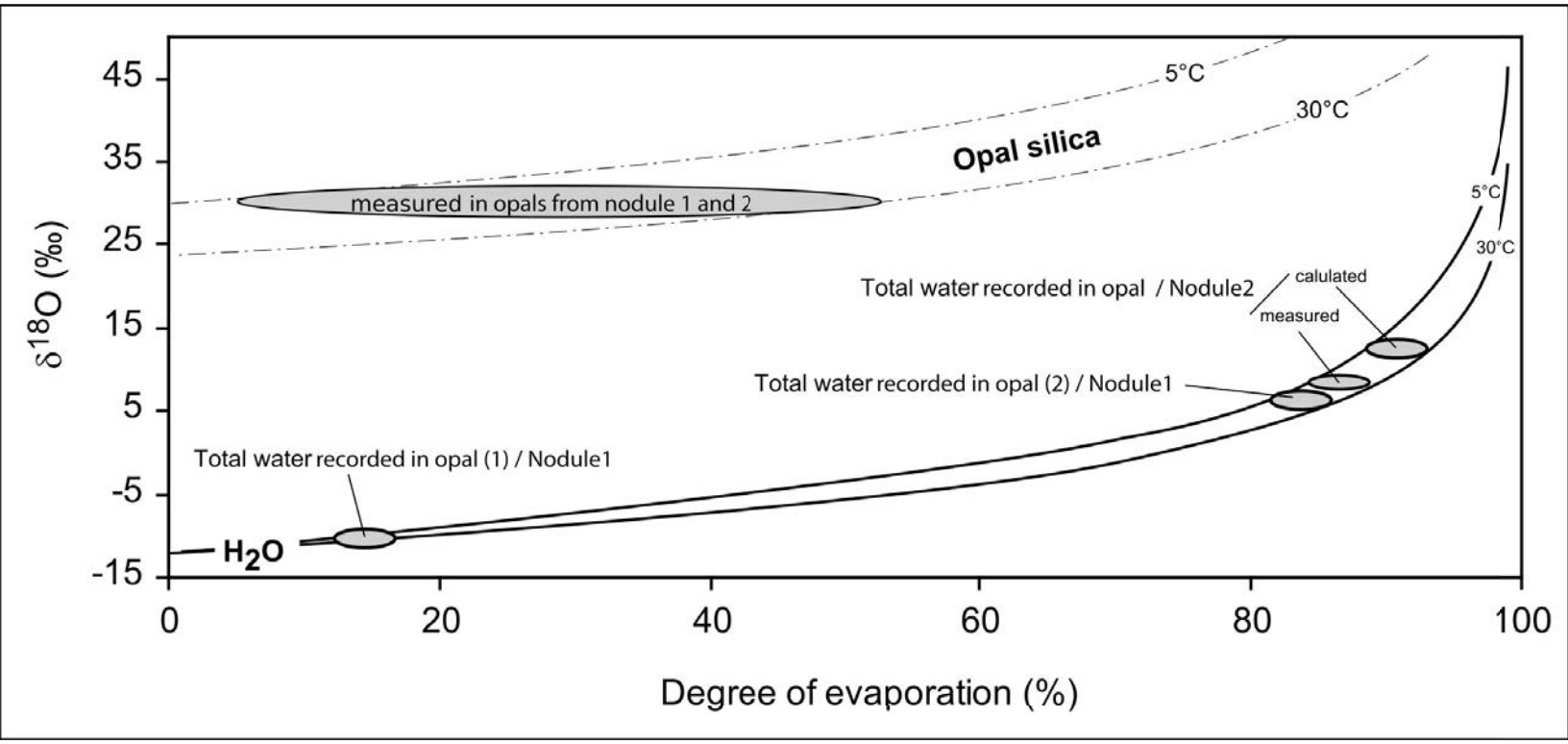
45
35
25
15
5
-5
-15
δ18O (‰)
0
20
40
60
80
100
Degree of evaporation (%)
5°C
30°C
Opal silica
measured in opals from nodule 1 and 2
5°C
30°C
Total water recorded in opal / Nodule2
calulated
measured
Total water recorded in opal (2) / Nodule1
Total water recorded in opal (1) / Nodule1
H2O